SCIENCE CHINA
Information Sciences

• RESEARCH PAPER •
Special Focus on Millimeter Wave Communications Techniques and Devices for 5G

August 2017, Vol. 60 080302:1–080302:11
doi: 10.1007/s11432-017-9127-6

Path loss model based on cluster at 28 GHz in the indoor and outdoor environments

Lai ZHOU[1,2,3], Limin XIAO[1,2,4], Zhi YANG[1,2,4], Jiahui LI[1,2,4], Jin LIAN[1,2,4] & Shidong ZHOU[1,2,4*]

[1]*State Key Laboratory on Microwave and Digital Communications, Tsinghua University, Beijing* 100084*, China;*
[2]*Tsinghua National Laboratory for Information Science and Technology, Tsinghua University, Beijing* 100084*, China;*
[3]*Department of Engineering Physics, Tsinghua University, Beijing* 100084*, China;*
[4]*Department of Electronic Engineering, Tsinghua University, Beijing* 100084*, China*

Received January 20, 2017; accepted May 4, 2017; published online June 30, 2017

Abstract This paper presents 28 GHz path loss model based on cluster obtained from channel measurement campaigns with rotating platforms and directional antennas in the indoor and outdoor environments. The transmitter (TX) and receiver (RX) both sweep a large range of angles in the azimuth and elevation plane on account of covering main propagation paths and measuring burden. As the sequence number of cluster increases, the path loss exponents (PLEs) increase while shadow factors also have a growing tendency. The PLE of all-clusters is the least because of multi propagation paths, and the LOS PLEs of corridor scenario are less compared with that of office scenario because of corridor's long and narrow structure. This improved model not only considers cluster characteristics, but also unites directional and omnidirectional models into the same framework, which to some extent improves the 5G mmWave channel model.

Keywords mmWave channel measurement, office and corridor, rotating platform, multipath components, path loss model based on cluster

Citation Zhou L, Xiao L M, Yang Z, et al. Path loss model based on cluster at 28 GHz in the indoor and outdoor environments. Sci China Inf Sci, 2017, 60(8): 080302, doi: 10.1007/s11432-017-9127-6

1 Introduction

Mobile communications in millimeter wave (mmWave) band have recently attracted a wide range interest with its huge frequency resource, which will take an important role in meeting the essential needs of high-data-rate and large-data-capacity in the modern society [1]. With the impending traffic growth and advancements in technology, there are some potential applications for mmWave to satisfy the capacity explosion, such as high-end wearables [2], high-speed railway [3] and unmanned aerial vehicles [4], and mmWave technology will help a lager number of mobile devices share data with each other or collect and send large data to the base station in the above application scenarios. Although there are some associated challenges when using mmWave, Ref. [5] shows that we can overcome the large attenuation of mmWave and make use of the abundant frequency resource in the 5G cellular networks based on the

* Corresponding author (email: zhousd@tsinghua.edu.cn)

result from propagation measurement campaigns. Ref. [6] studies the performance of outdoor mmWave ad-hoc networks and shows that mmWave can support high density and large spectral efficiency in the case of some blockages, resulting in much greater rate coverage than low frequency. Taking consideration of the demand in mmWave technology, fundamental knowledge of the channel characteristics is of great importance in 5G wireless communication system.

The mmWave has some special characteristics compared to the low frequency such as high attenuation and sparse multipath, and many channel measurement campaigns have recently been taken to have a deep understanding of the channel in different frequency bands and provide large data for channel modeling. New York University (NYU) wireless center acting as the pioneering research institution has used directional horn antenna to study channel characteristics of mmWave band in 28, 38, 73 GHz in the dense urban environment [5, 7]. Some famous research projects such as METIS and MiWEBA are also committed to take measurement campaigns and develop channel model for mmWave. What is more, ray-tracing (RT) technology is widely used in studying channel model because of high efficient simulation compared to time-consuming measurement [8, 9].

As we all know, the physical wireless channel has important effect on the communication and its reliability, and using accurate channel model is critical for the system design and evaluating protocol before actual performance. There are usually three kinds of channel models, deterministic model, statistical model, and the model with both features. RT model with detailed description of physical environment is the deterministic model. NYU wireless center proposed different kinds of pathloss model [10] and 3GPP-style model [11] based on large data from experiment and RT simulation, which both belong to statistical model. METIS model is the third model that combines map-based information to get lager-scale parameters and stochastic result to obtain small-scale parameters. Pathloss model related to the propagation distance is vital for system design, which is usually used to calculate the coverage area. To our best knowledge, there are few papers studying the pathloss model based on cluster, but clustering characteristic should be paid attention to because of sparse multipath in mmWave communication, especially for beamforming training and tracking technology [12].

In this paper, we take channel measurement campaigns in the mmWave band of 28 GHz to obtain as many omnidirectional channels in both azimuth and elevation plane as possible considering the trade off between experimental burden. A kind of efficient clustering method is proposed to cluster the multipath, then the strongest cluster usually consisted of line-of-sight (LOS) path could be distinguished from other clusters generated from reflecting or scattering mechanism. The path loss model based on different clusters in the indoor and outdoor environments not only considers the cluster characteristics, but also unites the directional and omnidirectional path loss models into the same framework. A part of the results (indoor environment) have been published in [13].

The remaining paper is structured as follows. Section 2 describes measurement system and experimental procedures, including different measurement environments. In Section 3, data processing and analysis methods are introduced. Section 4 represents the path loss model based on different clusters, then shows and compares the results of PLEs and shadow factors with NYU model based on similar environment. Section 5 summarizes the results and concludes this paper, and the future work is described at the end.

2 Measurement system and campaign

2.1 Measurement system description

In order to obtain omnidirectional channels in both azimuth and elevation, a pair of rotating platforms equipped with directional antenna were used to measure the 28 GHz wideband channel inside and outside the FIT building in Tsinghua University. The gain of horn antenna is 19.2 dBi with 20° and 18° half-power beamwidths (HPBWs) in the azimuth and elevation planes, respectively. The rotating platform acting as antenna support can move from −200 mm to 200 mm in X/Y axes; the scan range in the azimuth and elevation plane are [−180°, 180°] and [−90°, 90°], respectively. The vector network analyzer (VNA) was used to obtain channel impulse response (CIR), which was controlled by matlab software so that

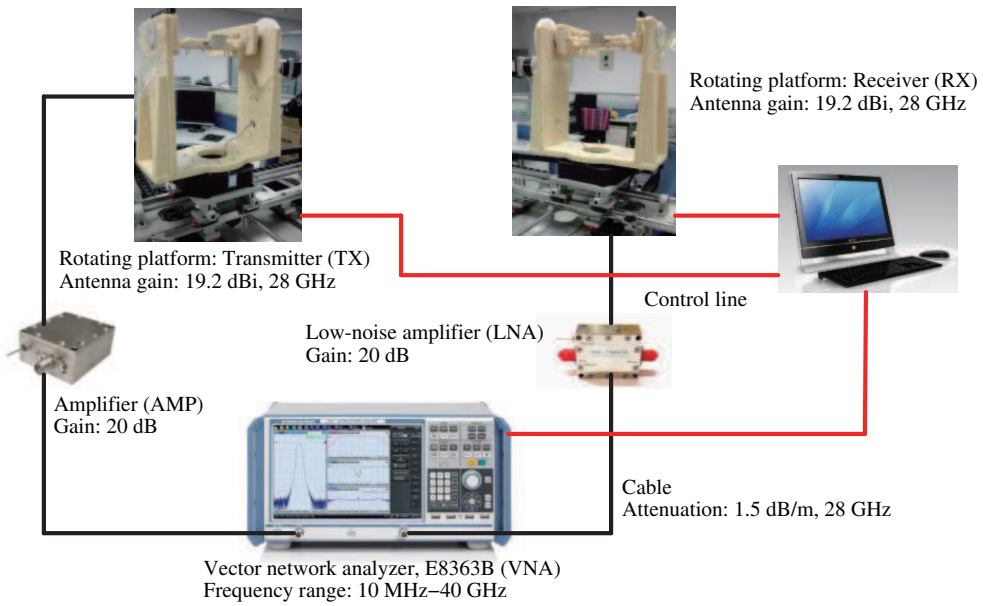

Figure 1 (Color online) Measurement system.

data could be recorded in the computer automatically when transmitter and receiver when conducting the scanning task. Wideband power amplifiers (AMP) with 20 dB gain and low-noise amplifiers (LNA) with 20 dB gain were used to improve the signal-noise ratio (SNA), and we choosed the number of AMP and LNA according to the practical need and measurement error caused by the components. The measurement system is shown in Figure 1.

In different measurement campaigns, we set bandwidth, sweep count in frequency-domain, sweep range in azimuth and elevation angle on account of practical environment and measuring burden, especially for the time-consuming scan at multi-angle. Taking the courtyard scenario for example, the bandwidth was 1 GHz, whose center frequency was 28 GHz; the sweep count was 2001, which implied a frequency interval of 0.5 MHz. Based on the above parameters, the measurable delay resolution was 1 ns, and the maximum measurable delay was 2000 ns, which implied that the maximum measurable distance was 600 m. As for the sweep range, we took the office scenario for example, the transmitter and receiver were both rotated 360° with the step increments of 10° in the azimuth plane, so that we could obtain omnidirectional channel response (36 angles × 36 angles) in two-dimensions. The main parameters of measurement system are summarized in Table 1.

2.2 Measurement environment and campaigns

We conducted the measurements inside and outside the FIT building of Tsinghua University; the environment included office room, corridor and courtyard. The directional horn antenna was fixed on the rotating platform at a height of 1.48 m above ground level, and antenna polarization was always vertical-to-vertical (V-V). As for the indoor environment, Figures 2 and 3 showed corresponding layouts of office and corridor scenario, respectively. Because there were many scattering paths from nearby objects in the office room, the TX and RX antenna were both rotated 360° in the azimuth plane with the step of 10°, while the sweep range was [−30°, 30°] in the corridor scenario covering the main propagation paths. The elevation angle was always fixed at 0° considering the practical need and measuring burden. As for the outdoor environment in Figures 4 and 5, the orientation of TX antenna was fixed to the middle of the courtyard while the height of TX was 6.7 m, and the RX antenna was rotated in both azimuth and elevation plane to emulate a practical outdoor cellular scenario. The similar omnidirectional channel response was obtained after capturing the majority of powerful multipath components. More details about the sweep procedure can be obtained in [13].

Table 1 Measurement system parameters

Parameter	Office	Corridor	Courtyard
Frequency	27–29 GHz	27–28 GHz	27.5–28.5 GHz
Bandwidth	2 GHz	1 GHz	1 GHz
Sweep count (frequency)	401	1001	2001
Frequency interval	5 MHz	1 MHz	0.5 MHz
Sweep range in azimuth plane (TX)	$[-180°, 180°]$	$[-30°, 30°]$	6°
Sweep range in elevation plane (TX)	0°	0°	−19.7°
Sweep range in azimuth plane (RX)	$[-180°, 180°]$	$[-30°, 30°]$	$[-180°, 180°]$
Sweep range in elevation plane (RX)	0°	0°	$[-20°, 20°]$
Step increment	10°	10°	10°
AMP number	1	1	1
LNA number	1/2	1	2
TX power	0 dBm	0 dBm	0 dBm

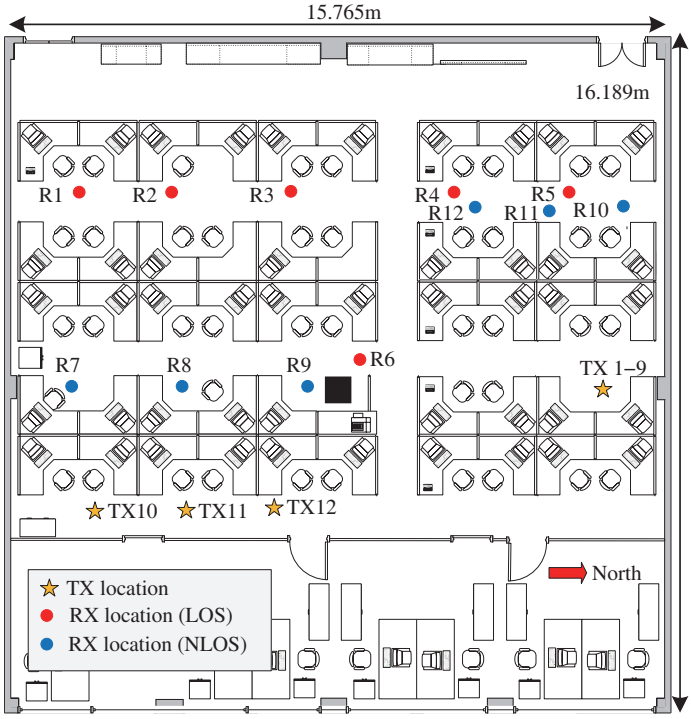

Figure 2 (Color online) Office scenario (4-408 room of FIT building, 15.765 m × 16.189 m × 2.789 m), there were 4 TX locations and 12 RX locations for a total of 12 TX-RX combination locations. In the NLOS situations, the LOS path was obstructed by the concrete pillars in the center of the room. There were objects such as concrete walls and pillars, glass walls and doors, wood doors and cupboard, plastic chairs and desks in the standard office scenario.

3 Data processing and analysis methods

3.1 SAGE algorithm

In order to calculate path loss based on cluster, there are two main steps to conduct, space-alternating generalized expectation-maximization (SAGE) algorithm and clustering method. The SAGE algorithm is an accurate and widely used method to extract multipath components (MPCs) such as complex amplitude, delay, angle of departure (AOD), angle of arrival (AOA) and doppler frequency shift in the field of channel measurement and modeling [14, 15].

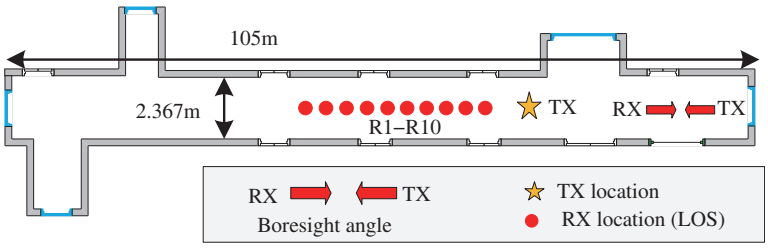

Figure 3 (Color online) Corridor scenario (the fourth floor of FIT building, 105 m × 2.367 m × 2.485 m), there were 1 TX location and 10 RX locations for a total of 10 TX-RX combination locations. There were objects such as concrete walls, glass windows and wood doors in the standard corridor scenario.

Figure 4 (Color online) Outdoor scenario (courtyard beside the FIT building, 50 m × 80 m), there were 1 TX location and 9 RX locations for a total of 9 TX-RX combination locations. The TX was fixed outside the window on the second floor of FIT building, and the orientation of horn antenna was 6° and −19.7° in the azimuth and elevation plane, respectively. There were objects such as concrete walls, glass windows, plastic chairs and desks, small trees and udershrub in the standard courtyard scenario.

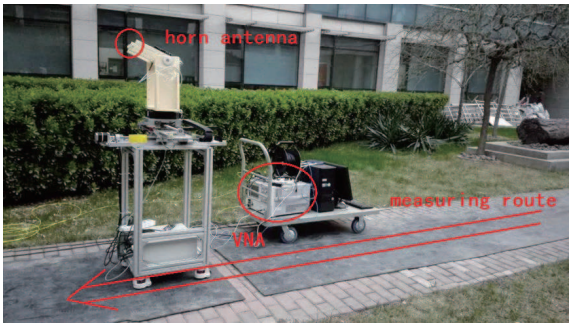

Figure 5 (Color online) Measuring route (the receiver moved along the route in the middle of the courtyard). 9 measuring positions were nearly uniformly distributed in this route whose distance was about 30 m. The sweep range of RX antenna was [−180°, 180°] and [−20°, 20°] in the azimuth and elevation plane, respectively.

Taking the office scenario for a example, the TX and RX antenna were rotated in different directions to establish a CIR matrix (36 × 36), which could be regarded as a virtual multiple-input and multiple-output (MIMO) with zero spacing between the array element. Assuming there are M and N elements in the TX and RX respectively, the received signal vector consisting of L paths can be written as

$$\boldsymbol{Y}(t) = [Y_1(t), \ldots, Y_N(t)]^{\mathrm{T}} = \sum_{l=1}^{L} \boldsymbol{s}(t; \Theta_l) + \sqrt{\frac{\mathrm{N}_0}{2}} \boldsymbol{N}(t), \tag{1}$$

where N_0 is a positive constant and $\boldsymbol{N}(t)$ is a standard N dimensional complex white Gaussian noise. $\boldsymbol{s}(t; \Theta_l)$ is the impinging wave contributed by the lth path, which can be expressed as

$$\boldsymbol{s}(t; \Theta_l) = [s_1(t; \Theta_l), \ldots, s_N(t; \Theta_l)]^{\mathrm{T}} = \alpha_l \boldsymbol{c}_R(\theta_{r,l}, \phi_{r,l}) \boldsymbol{c}_T(\theta_{t,l}, \phi_{t,l})^{\mathrm{T}} \boldsymbol{u}(t - \tau_l), \tag{2}$$

where $\Theta_l = [\alpha_l, \theta_{r,l}, \phi_{r,l}, \theta_{t,l}, \phi_{t,l}, \tau_l]$ is a vector of parameters of lth path to be estimated. α_l is the complex amplitude, $\theta_{r,l}$ and $\phi_{r,l}$ are AOAs in the azimuth and elevation plane, $\theta_{t,l}$ and $\phi_{t,l}$ are AODs in the azimuth and elevation plane, τ_l is the relative delay. $\boldsymbol{u}(t) = [u_1(t), \ldots, u_M(T)]^{\mathrm{T}}$ is the input signal vector, while M-dimensional vectors $\boldsymbol{c}(\theta, \phi)$ representing the response of virtual steering array to a wave impinging from (θ, ϕ) can be expressed as

$$\boldsymbol{c}(\theta, \phi) = [c_1(\theta, \phi), \ldots, c_M(\theta, \phi)]^{\mathrm{T}} = [f_1(\theta, \phi), \ldots, f_M(\theta, \phi)]^{\mathrm{T}}, \tag{3}$$

where $f(\theta, \phi)$ is the antenna radiation pattern.

3.2 Clustering method

A cluster is defined as a group of MPCs that have similar delays, AODs and AOAs in the azimuth and elevation plane [16]. Although there are some algorithms used to group estimated MPCs into clusters, such

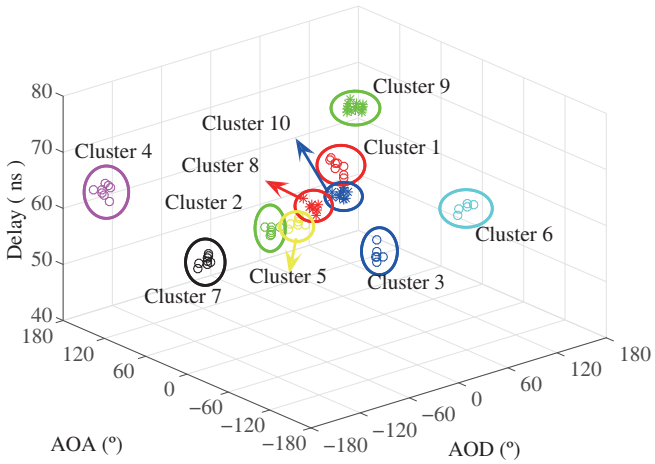

Figure 6 (Color online) Clustering the MPCs of 11th TX-RX combination location in the office (the clusters are sorted by power and cluster 1 is the strongest one among all of the clusters).

as K-means algorithm [17] and K-power-means algorithm [18], these algorithms need multiple iterations and bring larger computational burden when there are many parameters to be estimated. So we propose an efficient clustering method based on the cluster definition and the result is verified to be accurate compared with that of visual inspection. The main steps of clustering method are as follows.

Algorithm 1 Clustering method

Initialize the set of MPCs: $\Omega_n = \{\mathrm{MPC}_n(\alpha_n, \theta_{r,n}, \phi_{r,n}, \theta_{t,n}, \phi_{t,n}, \tau_n), n = 1, \ldots, L\}$.
for $i = 1$ to MAX **do**
  Choose the strongest path as the centroid of $\mathrm{Cluster}_i$: $\mathrm{MPC}_i = \max\{\mathrm{MPC}_n(\alpha_n), \mathrm{MPC}_n \in \Omega_n\}$,
  Choose the similar paths from group Ω_i as the element of $\mathrm{Cluster}_i$ based on MPC_i,
  if $n \in$ Case1 and $n \in$ Case2 **then**
    Case1: $\sqrt{(\theta_{r,n} - \theta_{r,i})^2 + (\phi_{r,n} - \phi_{r,i})^2 + (\theta_{t,n} - \theta_{t,i})^2 + (\phi_{t,n} - \phi_{t,i})^2} \leqslant \Delta\theta$,
    Case2: $\sqrt{\tau_n - \tau_i} \leqslant \Delta\tau$,
    $\{\mathrm{MPC}_n \in \Omega_n\} \subseteq \mathrm{Cluster}_i$,
  end if
  Obtain Ω_{i+1} after remove the $\mathrm{Cluster}_i$ from Ω_i and calculate the ratio: $e_i = \frac{P_i}{P_1} = \frac{\sum \alpha_n^2, \mathrm{MPC}_n \in \Omega_{i+1}}{\sum \alpha_n^2, \mathrm{MPC}_n \in \Omega_1}$.
  if $e_i \leqslant \varepsilon$ **then**
    go to end,
  else
    next i,
  end if
  Return: $\{\mathrm{MPC}_n(\alpha_n, \theta_{r,n}, \phi_{r,n}, \theta_{t,n}, \phi_{t,n}, \tau_n), \mathrm{MPC}_n \in \mathrm{Cluster}_i, i \leqslant \mathrm{MAX}\}$.
end for

There are some additional details for single step.

Ad 1) The number of MAX depends on practical environment, we can set 10 in the office scenario based on the visual inspection.

Ad 2) The value of $\Delta\theta$ and $\Delta\tau$ decide the size of cluster, we usually set $\Delta\theta = 20°$ and $\Delta\tau = 5$ ns based on the HPBWs of directional antenna.

Ad 3) The parameter ε acts as a threshold to remove the weak paths, which is usually set as 0.05.

Ad 4) The elements in the MPCs could be adjusted based on the scenario, and there are 4 elements in $\mathrm{MPC}_n(\alpha_n, \theta_{r,n}, \theta_{t,n}, \tau_n)$ at the office scenario.

Ad 5) The result is multi-cluster group of MPCs in each measurement position. Figure 6 shows 10 clusters of 11th TX-RX combination location (NLOS) in office scenario, and there are 5–15 rays in per cluster.

4 Path loss model based on cluster

There are two main kinds of path loss model to study the transmission characteristics of mmWave, omnidirectional path loss model and directional path loss model [10, 19]. The former one collect all the power from different directions, and the latter one is used to obtain the strongest path among the steerable angles, which is meaningful for beamforming and tracking. However, because there are a small number of propagation paths due to the sparse characteristic of mmWave, the cluster is usually used to describe and analyze the channel characteristics [16]. Based on the understanding of mmWave and the measurement result, we proposes the path loss model based on cluster, which not only considers the cluster characteristics of multipath, but also unites the omnidirectional and directional path loss model into the same framework.

Path loss model based on all clusters is similar to the omnidirectional model, which contains the main propagation clusters or paths with different AODs, AOAs and delays. Path loss model based on single cluster is similar to the directional model, but the improved model represents more information. The path loss model based on *Best-Cluster* represents the optimal propagation path between TX and RX. The path loss model based on *Second-Cluster* and *Third-Cluster* can be used to evaluate the channel situation in case of some blockages caused by moving obstacle, and these clusters act as backup paths to deal with the blockage. The path loss based on cluster is obtained as follows:

$$\mathrm{PL}(\mathrm{Cluster}_{\mathrm{all}}) = P_{TX} - 10\log_{10}\left[\sum_{i=1}^{L} P(\mathrm{Cluster}_i)\right], \tag{4}$$

$$\mathrm{PL}(\mathrm{Cluster}_i) = P_{TX} - 10\log_{10}\left[P(\mathrm{Cluster}_i)\right], \tag{5}$$

where P_{TX} is the transmit power in dBm, and L is the number of all clusters. $P(\mathrm{Cluster}_i)$ represents the power of ith cluster,

$$P(\mathrm{Cluster}_i) = \left|\sum_{n=1}^{N} \alpha_{n,i}\right|^2, \quad \mathrm{MPC}_n(\alpha_n, \theta_{r,n}, \phi_{r,n}, \theta_{t,n}, \phi_{t,n}, \tau_n) \in \mathrm{Cluster}_i, \tag{6}$$

where $\mathrm{MPC}_n(\alpha_n, \theta_{r,n}, \phi_{r,n}, \theta_{t,n}, \phi_{t,n}, \tau_n)$ represents multipath belonging to $\mathrm{Cluster}_i$, and $\alpha_{n,i}$ is the amplitude of nth path in the ith Cluster.

There are two kinds of methods to express the path loss model, the first one is close-in free space reference distance (CI) model [10] provided in (7),

$$PL_{\mathrm{CI}} = 10n\log_{10}(d/d_0) + 20\log_{10}(4\pi d_0/\lambda) + X_\sigma^{\mathrm{CI}}, \tag{7}$$

where $d_0 = 1$ m is the reference distance and d is the distance between TX and RX in 3D space, λ is the wave length of electromagnetic wave, n is the path loss exponent, and X_σ^{CI} is the shadow fading factor which is characterized as lognormal random variable with standard deviation σ. The second one is floating intercept (FI) model [10], which is expressed as

$$PL_{\mathrm{FI}} = 10n\log_{10}(d) + \beta + X_\sigma^{\mathrm{FI}}, \tag{8}$$

where β is the floating path loss intercept, X_σ^{FI} is the shadow fading factor similar with X_σ^{CI} in CI model. Although the CI model has physical basis and reasonable accuracy across many environments [20], we make the path loss model based on cluster with both methods, and minimum mean square error method (MMSE) is used to calculate the parameters.

Figures 7 and 8 show the 28 GHz LOS and NLOS path loss model based on cluster in the office scenario, while (a) shows CI model and (b) shows FI model. Taking the CI model for consideration, some PLEs are less than that of free space because of waveguide effect [10], where many clusters act as the propagation paths from different AODs, AOAs and delays reflected by glass door and concrete wall. The PLEs increase as the sequence number of cluster, occurring from the power of cluster decreasing as the

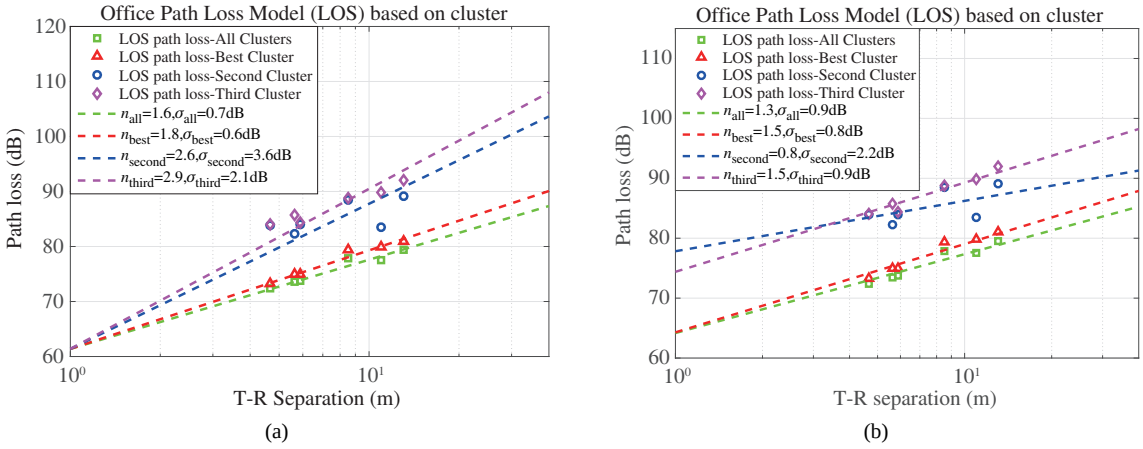

Figure 7 (Color online) 28 GHz path loss model (LOS) based on cluster in the office indoor environment. (a) CI model; (b) FI model.

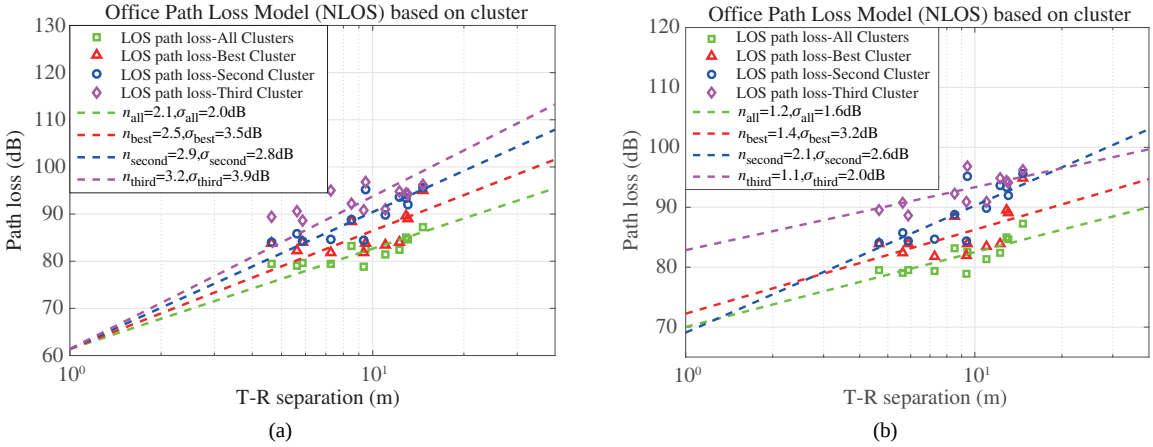

Figure 8 (Color online) 28 GHz path loss model (NLOS) based on cluster in the office indoor environment. (a) CI model; (b) FI model.

sequence number, which matches the situation that stronger cluster brings better communication service. As for the FI model without the reference intercept, the PLEs are usually less than that of CI model. Besides, the PLE of *Third-Cluster* with larger path loss is less than that of *Best-Cluster*, while the floating intercept increases as the sequence number of cluster, so the PLE on CI model just represents the increasing rate of path loss.

Figure 9 shows the 28 GHz LOS path loss model based on cluster in the corridor scenario. The shadow factors increase as the sequence number of cluster, the result matches the situation that worse propagation path has larger shadow fading. Besides, the PLEs of corridor scenario at LOS case are less compared with that of office scenario, because waveguide effect is more obvious in the long and narrow corridor.

Figure 10 shows the 28 GHz LOS path loss model based on cluster in the courtyard scenario. Compared with the PLEs in the indoor environment, the PLEs in the outdoor environment is larger because less clusters in the scenario, and there are just two clusters at most measuring positions, the LOS cluster and reflecting cluster from the ground. With the increase of the sequence number of cluster, the PLEs and shadow fading factors are both have an increasing tendency, and the PLEs of FI model are larger than that of CI model.

Table 2 summarizes the parameters of CI model and FI model in the indoor and outdoor environments. The parameters of omni-directional model and directional model at 28 GHz are also listed in the table for comparison, and the environment of measurement campaigns conducted by NYU wireless center is similar to ours [10, 20]. The PLEs for LOS case in the indoor and outdoor environments are in range

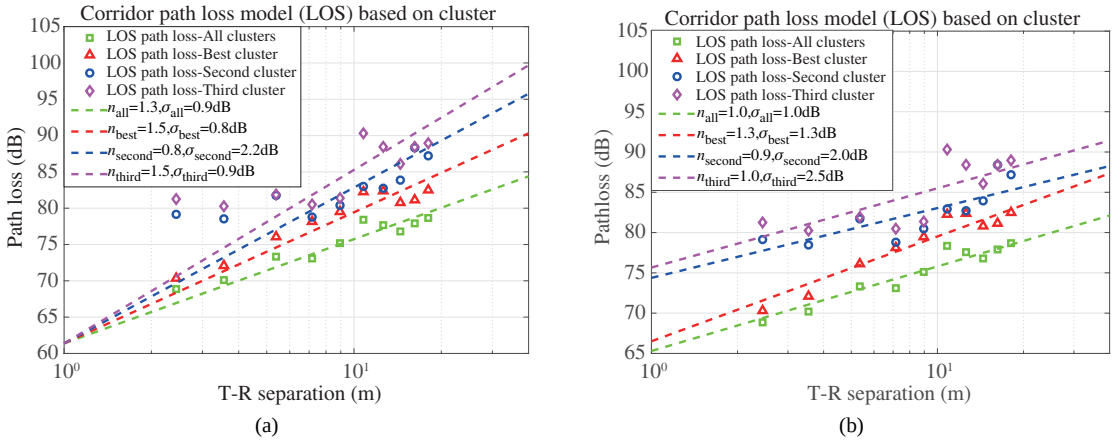

Figure 9 (Color online) 28 GHz path loss model (NLOS) based on cluster in the corridor indoor environment. (a) CI model; (b) FI model.

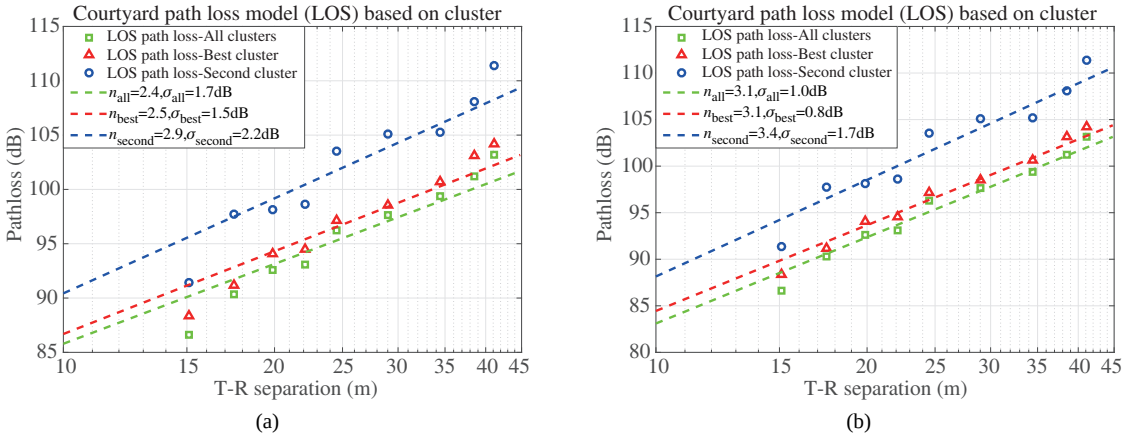

Figure 10 (Color online) 28 GHz path loss model (LOS) based on cluster in the courtyard outdoor environment. (a) CI model; (b) FI model.

Table 2 Comparison of the parameters between THU and NYU*

	Item		Omni-directional and all clusters					Directional and best cluster				
			n_{CI}	σ_{CI}	n_{FI}	β	σ_{FI}	n_{CI}	σ_{CI}	n_{FI}	β	σ_{FI}
THU	Indoor	LOS	1.6	0.7	1.3	64.2	0.9	1.8	0.6	1.5	64.3	0.8
		NLOS	2.1	2.0	1.2	70.0	1.6	2.5	3.5	1.4	72.2	3.2
	Outdoor	LOS	2.4	1.7	3.1	52.3	1.0	2.5	1.5	3.1	53.8	0.8
NYU	Indoor	LOS	1.1	1.8	1.2	60.4	1.8	1.7	2.5	1.0	68.3	2.0
		NLOS	2.7	9.6	3.5	51.3	9.3	3.0	10.8	3.7	54.1	10.7
	Outdoor	LOS	2.1	3.0	/	/	/	1.9	1.1	2.9	45.3	0.04

* THU: Tsinghua University; NYU: New York University.

of 1 to 2 and 2 to 3, respectively, and the values of NYU model are less than that of our model, which means that NYU model suffers from less path loss at LOS case. As for the NLOS case in the indoor environment, the PLEs and shadow factors of NYU model are both larger than our model. There is a possible explanation that TX and RX both rotated a wide range of angles such as 360° in the azimuth plane in our measurement, so that the communication situation is better due to many reflecting and scattering paths.

5 Conclusion

In this paper, the channel measurement campaigns are conducted with rotating platforms and directional antennas at 28 GHz mmWave band in the indoor and outdoor environments, such as office, corridor and courtyard scenario. The TX and RX both sweep a large range of angles in the azimuth and elevation plane on account of covering main propagation paths and measuring burden, then SAGE algorithm and an efficient clustering method are used to obtain the clusters of MPCs. The path loss model based on cluster is developed by using both the CI and FI model, and large scale characteristics including PLEs, shadow factors in LOS and NLOS cases are calculated and compared with that of NYU model in the similar environment.

For the result of our improved model based on CI model with respect to 1 m free space reference distance, as the sequence number of cluster increases, the PLEs increase while the shadow factors also have the growing tendency, occurring from the power of cluster decreasing as the sequence number, which matches the situation that stronger cluster brings better communication service and smaller shadow fading. Some PLEs are less than 2 in the office and corridor scenario because of waveguide effect, which have larger influence on the corridor with long and narrow structure. The propagation clusters in outdoor environment is less than that in the indoor environment, and the main clusters are from LOS and reflected paths. As for the comparison between our improved model and NYU model (directional and omnidirectional model), the PLEs and shadow factors of NYU model are both larger than our model at the NLOS case in the indoor environment, because we could obtain enough reflecting and scattering clusters. The path loss model based on different cluster not only considers the cluster characteristics, but also units the directional and omnidirectional path loss model into the same framework, which to some extent improves the 5G mmWave channel model. More study based on cluster will be carried out to solve the problems in the mmWave communication, such as small scale characteristics analysis, spatial and frequency consistency, and time variability.

Acknowledgements This paper was supported by National Basic Research Program of China (973) (Grant No. 2012CB316002), National High-tech R&D Program of China (863) (Grant No. 2015AA01A701), National Natural Science Foundation of China (Grant No. 61201192), Science Foundation for Creative Research Group of NSFC (Grant No. 61321061), National S&T Major Project (Grant No. 2017ZX03001011), MOST "Hongkong, Macau and Taiwan" Science Collaboration Project (Grant No. 2014AA01A707), Tsinghua-Qualcomm Joint Project.

Conflict of interest The authors declare that they have no conflict of interest.

References

1 Heath R W. Millimeter wave: the future of commercial wireless systems. In: Proceedings of IEEE Compound Semiconductor Integrated Circuit Symposium (CSICS), Austin, 2016. 1–4
2 Venugopal K, Heath R W. Millimeter wave networked wearables in dense indoor environments. IEEE Access, 2016, 4: 1205–1221
3 Song H, Fang X M, Fang Y G. Millimeter-wave network architectures for future high-speed railway communications: challenges and solutions. IEEE Wirel Commun, 2016, 23: 114–122
4 Xiao Z Y, Xia P F, Xia X G. Enabling UAV cellular with millimeter-wave communication: potentials and approaches. IEEE Commun Mag, 2016, 54: 66–73
5 Rappaport T S, Sun S, Mayzus R, et al. Millimeter wave mobile communications for 5G cellular: it will work! IEEE Access, 2013, 1: 335–349
6 Thornburg A, Bai T Y, Heath R W. Performance analysis of outdoor mmWave Ad Hoc networks. IEEE Trans Signal Process, 2016, 64: 4065–4079
7 Rangan S, Rappaport T S, Erkip E. Millimeter-wave cellular wireless networks: potentials and challenges. Proc IEEE, 2014, 102: 366–385
8 Schiavoni A, Leoni A, Arena D, et al. Ray tracing simulations at millimeter waves in different indoor and outdoor scenarios. In: Proceedings of 10th European Conference on Antennas and Propagation (EuCAP), Davos, 2016. 1–5
9 Hur S, Baek S, Kim B, et al. Proposal on millimeter-wave channel modeling for 5G cellular system. IEEE J Sel Top Signal Process, 2016, 10: 454–469
10 Maccartney R G, Rappaport T S, Sun S, et al. Indoor office wideband millimeter-wave propagation measurements and channel models at 28 and 73 GHz for ultra-dense 5G wireless networks. IEEE Access, 2015, 3: 2388–2424

11 Sun S, Rappaport T S, Thomas T A, et al. A preliminary 3D mm wave indoor office channel model. In: Proceedings of International Conference on Computing, Networking and Communications (ICNC), Garden Grove, 2015. 26–31
12 Wang J Y. Beam codebook based beamforming protocol for multi-Gbps millimeter-wave WPAN systems. IEEE J Sel Areas Commun, 2009, 27: 1390–1399
13 Zhou L, Xiao L M, Li J H, et al. Path loss model based on cluster at 28GHz in the office and corridor environments. In: Proceedings of IEEE 84th Vehicular Technology Conference (VTC-Fall), Montréal, 2016. 1–5
14 Fleury B H, Tschudin M, Heddergott R, et al. Channel parameter estimation in mobile radio environments using the SAGE algorithm. IEEE J Sel Areas Commun, 1999, 17: 434–450
15 Fleury B H, Jourdan P, Stucki A. High-resolution channel parameter estimation for MIMO applications using the SAGE algorithm. In: Proceedings of International Zurich Seminar on Broadband Communications, Access, Transmission, Networking, Zurich, 2002. 301–309
16 Gustafson G, Haneda K, Wyne S, et al. On mmWave multipath clustering and channel modeling. IEEE Trans Antennas Propag, 2014, 62: 1445–1455
17 Krishna K, Murty M N. Genetic K-means algorithm. IEEE Trans Syst Man Cybern, 1999, 29: 433–439
18 Czink N, Cera P, Salo J, et al. A framework for automatic clustering of parametric MIMO channel data including path powers. In: Proceedings of IEEE 64th Vehicular Technology Conference (VTC-Fall), Montréal, 2006. 1–5
19 MacCartney G R, Zhang J H, Nie S, et al. Path loss models for 5G millimeter wave propagation channels in urban microcells. In: Proceedings of IEEE Global Communication Conference (GLOBECOM), Atlanta, 2013. 3948–3953
20 Rappaport T S, MacCartney G R, Samimi M K, et al. Wideband millimeter-wave propagation measurements and channel models for future wireless communication system design. IEEE Trans Commun, 2015, 63: 3029–3056